

# Physical Principles of Self-Consistent Simulation of the Generation of Interface States and the Transport of Hot Charge Carriers in Field-Effect Transistors Based on Metal–Oxide–Semiconductor Structures

S. E. Tyaginov<sup>a,b</sup>, A. A. Makarov<sup>b</sup>, M. Jech<sup>b</sup>, M. I. Vexler<sup>a\*</sup>, J. Franco<sup>c</sup>, B. Kaczer<sup>c</sup>, and T. Grasser<sup>a</sup>

<sup>a</sup> Ioffe Institute, St. Petersburg, 194021 Russia

<sup>b</sup> TU Vienna, Institute for Microelectronics, Vienna 1040, Austria

<sup>c</sup> IMEC, Kapeldreef 75, 3001 Leuven, Belgium

\*e-mail: Vexler@mail.ioffe.ru

Submitted June 22, 2017; accepted for publication June 23, 2017

**Abstract**—A detailed simulation of degradation (caused by hot charge carriers) based on self-consistent consideration of the transport of charge carriers and the generation of defects at the SiO<sub>2</sub>/Si interface is carried out for the first time. The model is tested using degradation data obtained with decananometer *n*-type-channel field-effect transistors. It is shown that the mutual influence of the above aspects is significant and their independent simulation gives rise to considerable quantitative errors. In calculations of the energy distribution for charge carriers, the actual band structure of silicon and such mechanisms as impact ionization, scattering at an ionized impurity, and also electron–phonon and electron–electron interactions are taken into account. At the microscopic level, the generation of defects is considered as the superposition of single-particle and multiparticle mechanisms of breakage of the Si–H bond. A very important applied aspect of this study is the fact that our model makes it possible to reliably assess the operating lifetime of a transistor subjected to the effects of “hot” charge carriers.

DOI: 10.1134/S1063782618020203

## 1. INTRODUCTION

Surface states are always present at the insulator/silicon interface in a field-effect MIS (metal–insulator–semiconductor) transistor; these states can form charged defects. The presence of such defects gives rise to local distortions in the electrostatics of the device, which manifests itself, for example, in a shift of the threshold voltage of a field-effect transistor. These defects also affect the transport of electrons in the near-interface induced channel.

The surface concentration of traps ( $N_{it}$ ) can change with time in relation to the conditions of transistor operation. In fact, the evolution of the density of  $N_{it}$  governs the evolution (degradation) of the device characteristics. Typically, in experiments with degradation, higher (compared with those in the operation mode) voltages and temperatures are used. The main applied problem is prognostication of the operating lifetime specifically in the operating mode. The problem consists in the fact that, upon the transition from “hard” conditions of a stress on the device to “softer” operating voltages, the physical mechanisms responsible for transistor degradation can completely change [1–3], thus making the basic phenomenologi-

cal/empirical model invalid. Therefore, for the adequate simulation of degradation processes, it is necessary to provide an understanding and form an adequate description of the physical mechanisms corresponding to the real operating mode.

In annually published prognoses of the development of the electronics industry ITRS (International Technology Roadmap for Semiconductors), the task of increasing the reliability of the functioning of semiconductor devices is declared as an issue of paramount importance [4]. In addition, the main mode of damage of new-generation transistors is related to degradation of the gate insulator as caused by “hot” charge carriers. This is supported, for example, by recent studies performed by Intel Corp. [5, 6].

This study is devoted to detailed physical simulation of the processes of the formation of interface traps in a MIS structure; this simulation is performed simultaneously with that of variations in the kinetics of hot electrons in such a structure. At first, we present a model of defect generation in transistors based on the (silicon dioxide)/silicon (SiO<sub>2</sub>/Si) system. Then, we report the results of calculations of the trap density  $N_{it}$  for various conditions of a stress on the device. On the

basis of these data, we conclude that it is necessary to calculate self-consistently the density of the energy distribution for electrons and defects. The insulator/silicon interface is considered as a two-dimensional object; it is believed that it is sufficient to analyze variations only along the drain–source coordinate. Correspondingly, the density  $N_{it}$  becomes a function of the lateral coordinate  $x$  and time  $t$ , i.e.,  $N_{it} = N_{it}(x, t)$ .

## 2. MODEL OF THE FORMATION OF AN INTERFACE DEFECT IN THE COURSE OF DEGRADATION CAUSED BY “HOT” CHARGE CARRIERS

### 2.1. Possible Scheme of Defect Origination

As is known, the SiO<sub>2</sub>/Si interface is a disordered system [7]. Among other things, this manifests itself in the presence of dangling bonds Si–. These bonds can capture charge carriers, thus forming charged defects, referred to as  $P_b$  centers. In order to passivate free Si–bonds, hydrogen (H) is used; the latter is introduced directly during growth of the insulator film. Passive Si–H bonds are formed with the involvement of hydrogen. However, these bonds can be broken as a result of bombardment of the interface with hot charge carriers, which exactly represents the cause of degradation [8–10]. The surface density of passive Si–H bonds ( $N_0$ ) limits the concentration  $N_{it}$ . The value of  $N_0$  is determined by the specific technological process; as a rule, this value is in the range  $(5–7) \times 10^{13} \text{ cm}^{-2}$ .

Bond breakage occurs due to the combined effect of two processes, i.e., the single-particle process and multiple-particle process [2, 9–11]. The first process is initiated by a single hot charge carrier which can deliver (to the interface) the energy required for breakage of the bond (2.6 eV [12]) or even larger. This mechanism is dominant in devices with high voltages of stress/functioning and corresponds to “classical” degradation caused by hot charge carriers. However, in decanometer field-effect transistors (with low operating voltages), the concentration of hot charge carriers is low; as a result, multiparticle mechanisms become dominant [2, 11]. In this case, bombardment is performed by several “cold” particles, which gradually excite the bond; this excitation finally gives rise to the bond’s dissociation. For an adequate description of the bond-breakage reaction, it is necessary to consider all possible superpositions of the above mechanisms [13–16], which was exactly done in our model of degradation caused by hot charge carriers [15, 17]. The model also takes into account the interaction of a local electric field  $F(x, t)$  with the dipole moment of the Si–H bond [14, 15]. Such interaction brings about a decrease in the energy of bond breakage. Due to disorder at the SiO<sub>2</sub>/Si interface, this energy is a fluctuating quantity and is described by a normal

distribution, which is also taken into account in the model [14, 15].

### 2.2. Role of the Energy Distribution of Electrons

In simulation of the rates of both mechanisms, it is noteworthy to differentiate between “hot” and “cold” charge carriers [18]. This information is included in the generalized distribution function (DF) for charge carriers over energy  $f(E)\rho(E) = dn(E, x)/dE$  ( $\text{eV}^{-1} \text{ cm}^{-3}$ ). The generalized DF is the product of the probability of occupation of the state with the given energy  $f(E)$  by the density of states  $\rho(E)$ . Our model uses the ViennaSHE simulator [17], which performs deterministic solution of the Boltzmann equation. For each point  $x$  of the interface, the ViennaSHE calculates the DF for given structure of the device and voltages.

The distribution functions are then used in simulating the rate ( $\text{s}^{-1}$ ) of the dissociation of bonds by hot charge carriers [14, 15]:

$$I(E_a) = \int f(E)\rho(E)\sigma(E, E_a, d, F)v(E)dE + I_{\text{th}}. \quad (1)$$

Here,  $\sigma$  is the effective scattering cross section in the single-particle/multi-particle process and  $v(E)$  is the group velocity of charge carriers. The value of  $\sigma$  is affected, in addition to the energy  $E$ , by the binding energy  $E_a$ , its dipole moment  $d$ , and the value of the field  $F$ . The second term in (1) represents the rate of thermal activation of bond breakage. Integration is performed over the entire energy spectrum.

In the case of the excitation of a bond in the multiparticle process to the level  $i$  (see Fig. 1), the energy required for dissociation is effectively reduced by the value of the position of this level  $E_i$ . This is taken into account in calculation of the rate of dissociation of the excited bond:

$$I_i(E_a) = \int f(E)\rho(E)\sigma(E_{\text{eff},i})v(E)dE + \omega_{\text{th}} \exp\left(-\frac{E_{\text{eff},i}}{kT}\right). \quad (2)$$

The function  $\sigma(E_{\text{eff},i})$  is different from zero at a positive value of the energy  $E_{\text{eff},i}$ , which is calculated as  $E_{\text{eff},i} = E - E_a + E_i + dF$ , where the term  $dF$  represents the contribution of interaction of the dipole moment of the bond with the field. The factor  $\omega_{\text{th}}$  in (2) represents the “frequency of attempts” to attain thermally induced breakage,  $k$  is the Boltzmann constant, and  $T$  is the temperature of the lattice. The resulting rate of bond breakage is simulated as the superposition of the contribution of all levels, i.e.,

$$I(E_a) = \sum I_i(E_a). \quad (3)$$

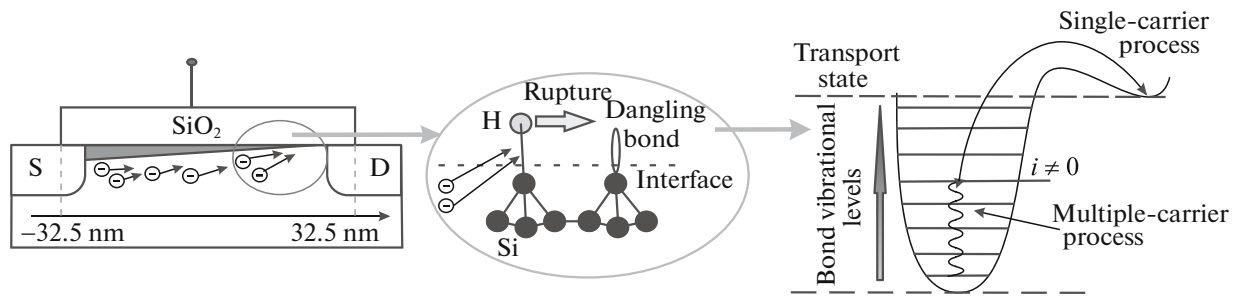


**Fig. 1.** Schematic representation of the mechanism of defect generation in the course of degradation caused by hot charge carriers. S stands for the source and D stands for the drain.

The energy  $E_a$  is a fluctuating quantity, which also should be taken into account in the course of determining the rates of bond breakage:

$$I = \int I(E_a) \Gamma(E_a, \langle E_a \rangle, \delta_a) dE_a. \quad (4)$$

Here,  $\langle E_a \rangle$  is the mean value of the breakage energy,  $\delta_a$  is its standard deviation, and  $\Gamma(E_a, \langle E_a \rangle, \delta_a)$  is the density of the normal distribution.

The incorporated defects affect the electrostatics of the device by changing the profile of the field  $F(x, t)$  and of the potential in the structure. Simultaneously, the mobility of charge carriers decreases. As a consequence, the form of the DF appearing in (1) also becomes distorted. Therefore, for correct simulation of the degradation caused by hot charge carriers, it is necessary to perform a self-consistent calculation of the rates of defect generation and of the distribution functions for charge carriers with respect to energy.

### 3. RESULTS OF CALCULATIONS IN THE CONTEXT OF THE MODEL AND DISCUSSION

The self-consistent simulation of the transport of charge carriers and of the kinetics of defect generation is a rather resource-consuming task; therefore, in our previous model, the set of DFs for different coordinates  $x$  was calculated only once for  $t = 0$  [14, 15, 19]. In this study, we take a step forward: we estimate the effect of built-in defects on the distribution function for charge carriers. The estimates are performed for decananometer transistors with a gate length of 65 nm and with silicon oxynitride (SiON) as the gate insulator (the physical thickness of the layer is 2.5 nm).

#### 3.1. Software Resources for Simulation

The ViennaSHE simulator used by us for determining the DFs, expands them into series of spherical harmonics [17]. The simulator includes the effects of the real band structure of Si for electrons/holes up to high energies. The ViennaSHE simulator takes into account such mechanisms of scattering as impact ionization, scattering at a charged impurity, surface scat-

tering, and electron–phonon and electron–electron interactions. The last type of interaction is found to be the main factor of degradation caused by hot charge carriers in transistors with a channel length of  $< 120$  nm [20, 21].

#### 3.2. Preliminary Estimate of the Effect Scale

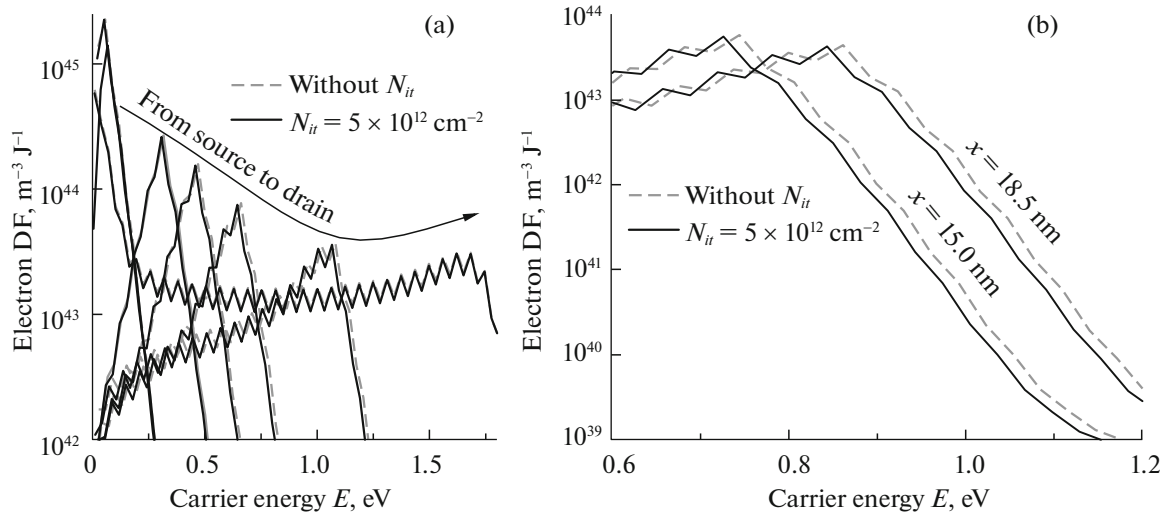
With the aim of preliminary estimation of the scale of defect effect on the DF, we performed a comparatively simple calculation with the given constant value  $N_{it} = 5 \times 10^{12} \text{ cm}^{-2}$  in the presumed case if defects with the given density are homogeneously distributed along the interface. This is, however, an artificial example: in practice, degradation caused by hot charge carriers is a highly inhomogeneous phenomenon and the  $N_{it}$  profiles feature a pronounced peak near the cutoff point of the transistor [8, 9, 22].

Figure 2 shows a series of DFs calculated at  $V_{ds} = V_{gs} = 1.8 \text{ V}$  ( $V_{ds}$  and  $V_{gs}$  are the drain–source and gate–source voltages, respectively) and at the temperature  $T = 25^\circ\text{C}$ . It can be seen that the incorporation of interface states changes radically the shape of distributions, especially, the occupation of their high-energy tails. The effect is most significant for regions closer to the drain: for example, at the lateral coordinates  $x = 15.0$  and  $18.5 \text{ nm}$ , the occupation numbers decrease by two–three times. It can be concluded from Fig. 2 that the presence of quite conventional concentrations of defects radically changes the DF.

#### 3.3. Procedure of Quantitative Calculation

As was already noted, the self-consistent description of the above process is necessary for accurate estimation of the degree of the effect of defect incorporation on the transport of charge carriers. In addition, for calculating the DF at some point with the coordinate  $x$  at the interface, we are bound to have the value of  $N_{it}$  not only at this point but also at all points at the interface.

The general algorithm can be described as follows. At the initial moment, it is assumed that  $N_{it}(x, 0) = 0$ .



**Fig. 2.** Series of distribution functions (DFs) for electrons with respect to the energy  $E$ ; the functions are calculated taking into account or disregarding the effect of  $N_{it}$ .  $V_{ds} = V_{gs} = 1.8 V$  and  $T = 25^\circ C$ . (a) Representation of the evolution of both families with the lateral coordinate. (b) Representation of the DFs for the coordinates ( $x = 15.0 nm$  and  $18.5 nm$ ) and energies at which the effect is most significant. The source corresponds to  $x = -32.5 nm$  and the drain corresponds to  $x = 32.5 nm$ .

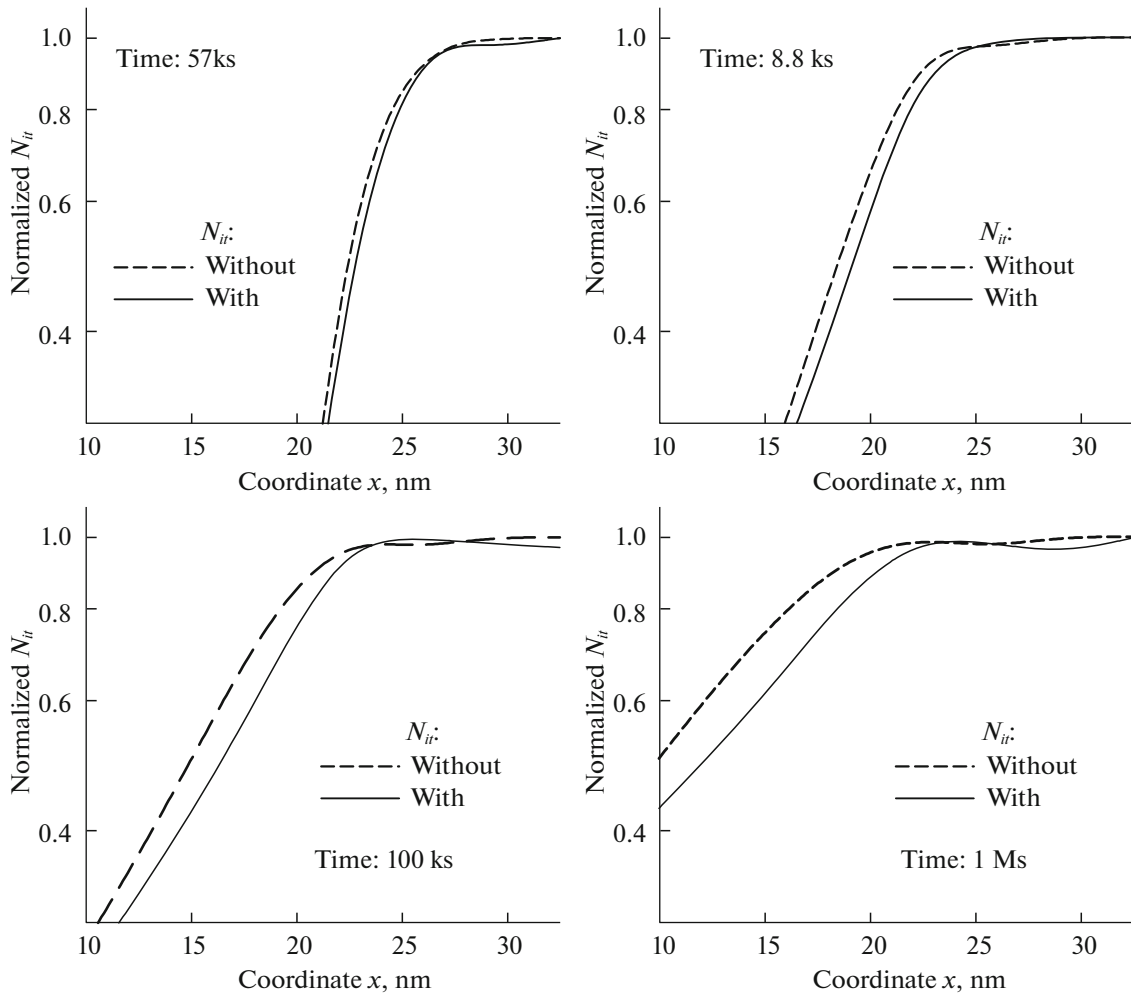


**Fig. 3.** Profiles for the concentration of traps at the interface,  $N_{it}(x)$ , as calculated taking into account and disregarding the effect of incorporated defects on the transport of charge carriers in the transistor. Only the values of  $N_{it}$  in the region of the maximum (in the vicinity of the cut-off point of the field-effect transistor) are shown.

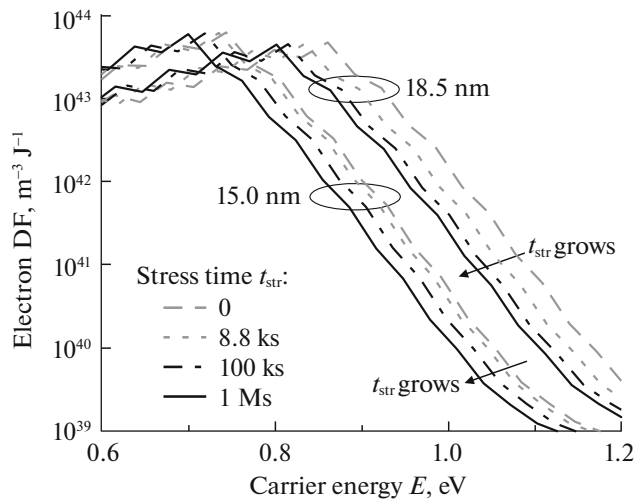


**Fig. 4.** Family of electron distribution functions (DFs) calculated taking into account and disregarding the real profiles of the surface concentration of defects  $N_{it}$  for several steps in time (stress time  $t_{str}$ ). The data on DFs are presented for those values of the lateral coordinate for which the effect is most pronounced.  $V_{ds} = V_{gs} = 1.8$  V,  $T = 25^\circ\text{C}$ .

For any moment  $t$ , the distributions of the potential and electric field  $F(x, t)$  are calculated first of all by solving the Poisson equation. This makes it possible to calculate the DFs for different coordinates at a given moment of time. Using the DF, we determine the rate of defect generation  $I$  (see formulas (1)–(4)), which, after multiplication by  $N_0$  and by the step in time, produces the value of the new density of traps:  $N_{it}(x, t + \Delta t) = N_{it}(x, t) + N_0 I(x, t) \Delta t$ . This procedure is repeated cyclically using the already corrected value of  $N_{it}$  for the next moment in time.

### 3.4. Examples of Precise Estimation of the Influence of Defects

We now provide examples illustrating the role of defects in the context of the above-described algorithm with self-consistency taken into account. For comparison (without self-consistency), we use the results of calculation, at which we calculate the DFs at all steps in time for the zero value of  $N_{it}$ , i.e., disregarding the fact of evolution of defects' density.

Figure 3 shows the calculated profiles of the quantity  $N_{it}(x, t)/N_0$  at four moments in time (only the region closer to the drain is shown; in this region, the effects of hot electrons are most profound). We can see that the differences between results become more pronounced with time. Variations in  $N_{it}(x, t)$  are due to changes in the distribution function for electrons and the electric-field strength  $F(x, t)$  with time. Also, in the version without self-consistency, the calculation of

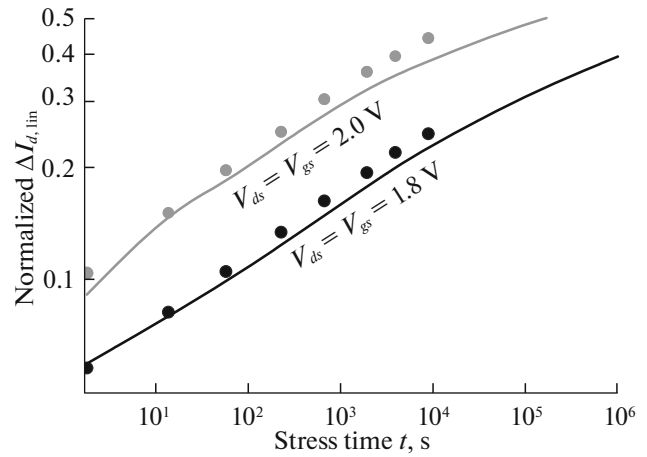


**Fig. 5.** Relative changes in the drain current (linear mode) with time,  $\Delta I_{d,lin}(t)$ , in the course of degradation caused by hot charge carriers for two conditions of stress. Points represent experimental data and continuous lines are drawn according to the results of simulation with the effect of  $N_{it}$  taken into account.

the DF is inaccurate, which specifically gives rise to the discrepancy.

Figure 4 shows two families of DFs, which were derived for the same lateral coordinates as in Fig. 2, for different values of the degradation time ( $t = 0$  corresponds to a “fresh” device with  $N_{it} = 0$ , i.e., without self-consistency). It can be seen that, due to the effect of increasing  $N_{it}$ , the occupancy can vary significantly, especially at long times of degradation. This indicates that the effect under consideration cannot be disregarded and the self-consistent description of the process of defect generation and of the transport of charge carriers is necessary.

### 3.5. Conformity with the Experimental Data

A straightforward comparison of the experimental and calculated data is unfeasible since the distribution functions cannot be measured directly. However, it is possible to verify the model by comparing the evolution of the drain current in a field-effect transistor subjected to the effect of hot charge carriers.

As an indicator of degradation, we use the relative change in the linear drain current  $\Delta I_{d,lin}(t) = (I_{d,lin}(t) - I_{d,lin0})/I_{d,lin0}$ , where  $t$  is the time of degradation and  $I_{d,lin0}$  is the drain current of a transistor, which is not subjected to the effect of hot charge carriers. The current in the linear mode corresponds to the drain-source and gate-source voltages  $V_{ds} = 0.05$  V and  $V_{gs} = 1.5$  V, respectively. Figure 5 shows the dependences  $\Delta I_{d,lin0}$  under two conditions:  $V_{ds} = V_{gs} = 1.8$  V and 2.0 V (at a temperature of  $25^\circ\text{C}$ ). The calculated dependences  $\Delta I_{d,lin}(t)$  were obtained with the effect of

$N_{it}$  on the distribution functions of electrons taken into account. However, it should be emphasized that attainment of as close as possible correspondence between the results of calculations of the drain currents and experimental data was not the task of this study. The aim of this study was estimation of the scale of the effect of increasing concentration  $N_{it}$  on the distribution functions and, as a consequence, on the characteristics of degradation (Figs. 2–4). The main conclusion following from Fig. 5 is that the used model does not result in large discrepancies with the experiment in the considered cases; this is indicative of the adequacy of our approach and of the theoretical results shown in Figs. 3–5.

#### 4. CONCLUSIONS

We analyzed the effect of the generation of interface states on the energy distribution functions of electrons in the course of degradation of a field-effect transistor as caused by hot charge carriers. Analysis was performed using the degradation model suggested by us; in this model, single-particle and multi-particle mechanisms of breakage of the silicon–hydrogen bond, interaction of the field in the insulator with the dipole moment of the bond, and also the statistical spread of the binding energy are taken into account. Calculations of the rates of dissociation were based on simulation of the transport of charge carriers taking into consideration the real band structure of silicon and various mechanisms of scattering (including electron–electron interactions).

It is shown by us that the accuracy of calculation of the DFs used in analysis of the process of defect generation can affect profoundly both the predicted profile of the trap concentration at the  $\text{SiO}_2/\text{Si}$  interface and such characteristics of the device as the linear current of the drain. In turn, the role of traps as the factor determining the form of distribution functions for electrons increases with time. In general, the results show that the mutual influence of the transport of charge carriers and the formation of defects is very important. Self-consistent consideration of these two aspects is required for correct description and simulation of this type of degradation.

#### REFERENCES

1. W. McMahon, A. Haggag, and K. Hess, *IEEE Trans. Nanotech.* **2**, 33 (2003).
2. A. Bravaix, C. Guerin, V. Huard, D. Roy, J. Roux, and E. Vincent, in *Proceedings of the International Reliability Physics Symposium IRPS, 2009*, p. 531.
3. K. Hess, L. F. Register, B. Tuttle, J. Lyding, and I. C. Kizilyalli, *Physica E* **3**, 1 (1998).
4. *International Technology Roadmap for Semiconductors ITRS* (2015), Chap. 5.
5. S. Novak, C. Parker, D. Becher, M. Liu, M. Agostinelli, M. Chahal, P. Packan, P. Nayak, S. Ramey, and S. Natarajan, in *Proceedings of the 2015 IEEE International Reliability Physics Symposium, 2015*, p. 2F.2.1.
6. S. Ramey, Y. Lu, I. Meric, S. Mudanai, S. Novak, C. Prasad, and J. Hicks, in *Proceedings of the 2015 IEEE International Integrated Reliability Workshop IIRW, 2015*, p. 56.
7. C. R. Helms and E. H. Poindexter, *Rep. Prog. Phys.* **57**, 791 (1994).
8. A. Bravaix and V. Huard, in *Proceedings of the European Symposium Reliability of Electron Devices Failure Physics and Analysis ESREF, 2010*, p. 1267.
9. S. Rauch and G. L. Rosa, in *Proceedings of the International Reliability Physics Symposium IRPS, 2010*.
10. S. Tyaginov and T. Grasser, in *Proceedings of the International Integrated Reliability Workshop IIRW, 2012*, p. 206.
11. W. McMahon and K. Hess, *J. Comput. Electron.* **1**, 395 (2002).
12. K. L. Brower, *Phys. Rev. B* **42**, 3444 (1990).
13. S. E. Tyaginov, I. A. Starkov, O. Triebel, J. Cervenka, C. Jungemann, S. Carniello, J. M. Park, H. Enichlmair, M. Karner, C. Kernstock, E. Seebacher, R. Minixhofer, H. Ceric, and T. Grasser, in *Proceedings of the International Symposium on the Physical and Failure Analysis of Integrated Circuits IPFA, 2010*.
14. M. Bina, S. Tyaginov, J. Franco, Y. Wimmer, D. Osinstev, B. Kaczer, T. Grasser, et al., *IEEE Trans. Electron Dev.* **61**, 3103 (2014).
15. S. Tyaginov, M. Jech, J. Franco, P. Sharma, B. Kaczer, and T. Grasser, *IEEE Electron Dev. Lett.* **37**, 84 (2016).
16. P. Sharma, S. Tyaginov, M. Jech, Y. Wimmer, F. Rudolf, H. Enichlmair, J.-M. Park, H. Ceric, and T. Grasser, *Solid State Electron.* **115** (pt. B), 185 (2016).
17. M. Bina, K. Rupp, S. Tyaginov, O. Triebel, and T. Grasser, in *Proceedings of the International Electron Devices Meeting IEDM, 2012*, p. 713.
18. S. Tyaginov, I. Starkov, C. Jungemann, H. Enichlmair, J. M. Park, and T. Grasser, in *Proceedings of the European Solid-State Device Research Conference ESSDERC, 2011*, p. 151.
19. S. Tyaginov, I. Starkov, O. Triebel, H. Enichlmair, C. Jungemann, J. M. Park, H. Ceric, and T. Grasser, in *Proceedings of the International Conference on Simulation of Semiconductor Processes and Devices SISPAD, 2011*, p. 123.
20. S. E. Rauch, F. J. Guarin, and G. LaRosa, *IEEE Electron Dev. Lett.* **19**, 463 (1998).
21. P. Sharma, S. Tyaginov, S. E. Rauch, J. Franco, A. Makarov, M. I. Vexler, B. Kaczer, and T. Grasser, *IEEE Electron Dev. Lett.* **38**, 160 (2017).
22. S. Tyaginov, I. Starkov, H. Enichlmair, J. M. Park, C. Jungemann, and T. Grasser, *ECS Trans.* **35**, 321 (2011).

*Translated by A. Spitsyn*